

Low-lying excitation spectrum of quantum many-body systems

P. Monthoux

Department of Physics and National High Magnetic Field Laboratory, Florida State University, Tallahassee, Florida 32306

E. Manousakis

Department of Physics and Center of Materials Research and Materials, Florida State University, Tallahassee, Florida 32306

(Received 12 February 1996; revised manuscript received 24 July 1996)

We present a numerical method for calculating the ground state correlations and low-lying excitations in a discrete and finite many-body system. The method combines the advantages of real space and momentum space renormalization group ideas and is similar in many respects to the correlated basis functions perturbation theory, but is nonperturbative in nature. To illustrate the method, we apply it to the one-dimensional Heisenberg antiferromagnetic spin- $\frac{1}{2}$ chain. [S0163-1829(96)09445-3]

INTRODUCTION

The numerical methods currently in use to tackle the quantum many-body problem of condensed matter systems have some drawbacks. Using exact diagonalization techniques, one expresses the Hamiltonian matrix in a conveniently chosen many-body basis; such calculations can only be performed for very small-size systems due to the exponential growth of the size of the matrix with the system size. Quantum Monte Carlo techniques which overcome this difficulty by sampling only the important part of the Hilbert space are best suited for ground state and finite-temperature properties of bosonic systems. Using such methods it is very difficult to extract information about the ground state or excited states of fermion systems because of the “fermion sign problem.”

The renormalization group (RG) method was introduced by Wilson¹ and was very successfully used to obtain the low-lying excitations in the Kondo problem. This technique overcomes the problem of the exponential growth of the Hilbert space by carefully selecting the states kept at each iteration and can be used for either bosonic or fermionic systems. Shortly after Wilson's solution to the Kondo problem real space RG methods were applied to quantum lattice models.² While good results were generally obtained for the total ground state energy of the system, the ground state wave function was not well described. More recently a density matrix RG algorithm was proposed and performed very well in the case of one-dimensional (1D) lattice models.³ However, this method uses critical features of the 1D lattice and the prospects for applying the technique in higher dimensions are not very good.

In the real space RG approach it is very difficult to describe correlations existing over a length scale greater than the block size. This led some authors to propose RG transformations in momentum space.^{4,5} In these calculations the low-lying excitation energies and long-range correlations are well described; however, the short-range correlations and the correlation energy is not described accurately, as expected.

In this paper we present a method which combines the advantages of real space RG ideas to describe the short-range correlations and of momentum space RG ideas for an accu-

rate description of the long-range correlations. We must first take care of the short-range correlations in the ground state, since these correlations contribute the most to the energy. Moreover, we expect that these short-range correlations can be described rather accurately by incorporating a relatively small part of the entire Hilbert space because of their local nature. To this end, we make use of techniques developed in the context of quantum chemistry.⁶ An adaptive state selection algorithm is used to select a set of many-body basis functions that yields as low a variational ground state energy as possible, given the constraint on the number of such basis states that can practically be handled. To obtain a satisfying solution to the problem we must also describe the low-lying excitation spectrum and long-range correlations accurately. Thus we define a set of correlated basis functions obtained by acting with suitable correlation operators on a few low-lying states found in the previous step which generate long wavelength low-lying excitations. We proceed by performing a variational calculation in the subspace spanned by the correlated states. This step can also correct the long distance behavior of the correlation functions. Furthermore, we expect the intermediate correlations to interpolate smoothly between the short-range and long-range correlations which have been described accurately. The present method resembles the correlated basis functions perturbation theory (CBFPT) which has been successfully applied to study ground state and low-lying excitations in liquid helium.⁷ In CBFPT one defines a set of correlated states and expresses the Hamiltonian in this basis. The diagonal part of the Hamiltonian is used as the unperturbed piece H_0 and the off-diagonal part of the Hamiltonian is treated by perturbation theory. CBFPT works because the short-range correlations are taken into account in H_0 . The difference between the exact energy and the ground state energy of H_0 is small and can be accounted for by low-order perturbation theory. Our approach can be viewed as a numerical implementation of the ideas behind CBFPT but is nonperturbative and variational. In addition, the CBFPT is a semianalytic method which involves an approximate calculation of the matrix elements of the Hamiltonian whereas in the present method they are calculated exactly.

DESCRIPTION OF SHORT-RANGE CORRELATIONS

We wish to illustrate the method on a simple model problem, the 24-site Heisenberg spin- $\frac{1}{2}$ chain with periodic boundary conditions. Our method does not depend in any critical way on the dimensionality of the problem, but 1D systems are stringent tests, since the quantum fluctuations are especially strong in one dimension. The Hamiltonian is

$$H = J \sum_{i=1}^N \{S_i^z S_{i+1}^z + \frac{1}{2}(S_i^+ S_{i+1}^- + S_i^- S_{i+1}^+)\}, \quad (1)$$

where $N=24$ and $S_{N+1}^\alpha \equiv S_1^\alpha$, $\alpha=z, \pm$.

Our goal is to describe well both the ground state correlations and the low-lying excitations. To achieve this, one must describe short-range and long-range correlations equally well. Our method thus consists of two steps. In the first step, we wish to obtain as good short-range correlations as is possible given the necessarily limited computer resources. These short-range correlations must be treated first since they contribute most of the energy, and this is best done in real space. Therefore, we chose to work with the real space basis:

$$\{|m\rangle\}_{i=1}^{2^N} = \{|\sigma_1, \sigma_2, \dots, \sigma_N\rangle\}_{\sigma_i=\uparrow, \downarrow} \quad (2)$$

or what is equivalent, our reference Hamiltonian H_0 , which is diagonal in that basis, is $H_0 = \sum_{i=1}^N S_i^z S_{i+1}^z$. It is clear that the ultimate accuracy of the method depends on a good choice of the reference Hamiltonian H_0 . However, as our results demonstrate, our approach gives good results even when the mean-field or classical reference Hamiltonian H_0 is a relatively poor starting point as is the case here. We would expect this choice to be much better in higher dimensions, where a mean-field can give a qualitatively correct description of the ground state.

In order to reduce the number of states one has to keep track of, it is advisable to make use of the symmetries of the Hamiltonian. We have used translation invariance and conservation of total z component of the spin, but have ignored parity, for simplicity. Moreover, we will consider only the zero magnetization ($S_z^{\text{tot}}=0$, equal number of up and down spins) and the zero total momentum sector ($k=0$). In what follows, the number of states mentioned is the number of inequivalent basis functions under these two symmetry operations in the $S_z^{\text{tot}}=0$, $k=0$ sector. Our basis states $\{|n\rangle\}$ for this symmetry sector are thus linear combinations of the states $\{|m\rangle\}$ in Eq. (2).

The states $\{|n\rangle\}$ are now classified relative to their matrix elements $\langle n|H_0|n\rangle \equiv E_n$. The Néel state $(1/\sqrt{2})\{|\uparrow\downarrow\uparrow\downarrow, \dots, \uparrow\downarrow\rangle + |\downarrow\uparrow\downarrow\uparrow, \dots, \downarrow\uparrow\rangle\}$ is the lowest energy state, with $E_{\text{Néel}} = -6J$ [each antiferromagnetic bond contributes $-(J/4)$ and there are 24 of them]. From now on we shall use units where $J=1$. The excited states are obtained by flipping an even (to conserve S_z^{tot}) number of spins. The states just above the Néel state have two nearest neighbor spins flipped, namely two ferromagnetic bonds costing each an energy of $\frac{1}{2}$. Their total energy is thus -5 . The next highest states have four ferromagnetic bonds, and so on. The number of states and their energy relative to H_0 are given in Table I. It is important to realize that the states in adjacent

TABLE I. States and their energy relative to H_0 .

Energy	Number of states
-6	1
-5	11
-4	305
-3	3027
-2	13626
-1	30492
0	35594
1	21780
2	6813
3	1009
4	61
5	1

entries in Table I can be obtained from one another by local transformations, since they differ in energy by 1.

Next, we first retain all the states below or at a certain energy cutoff E_c and diagonalize the full Hamiltonian H in that restricted subspace. All the diagonalizations in this work were carried out with the Davidson algorithm.⁸ To the extent that the eigenstates of the mean-field Hamiltonian give an accurate representation of the local correlations in the true many-body ground state, and in the absence of any other information about the ground state correlations, this is a reasonable selection of the states to keep in order to describe the short-range correlations in the system. But since our choice of states ignores the effect of the off-diagonal Hamiltonian matrix elements, it is clearly not optimal. However, after the diagonalization of the full Hamiltonian in that restricted subspace, we do have some information about the effect of off-diagonal matrix elements. We use this information to improve on our first guess to find a better set of configurations to describe the short-range correlations in the system. We must contend ourselves with an approximate solution to the problem of finding the best N_s configurations out of the $N_{\mathcal{H}}$ configurations in the full Hilbert space, since an exact answer to this combinatorial optimization problem is of course out of the question. We thus make use of the clever basis set reduction and state selection techniques developed in quantum chemistry.⁶ It is important to realize that one must choose the N_s spin configurations to describe the short-range correlations in an adaptive fashion, since whether or not one should keep a certain configuration $|\alpha_i\rangle$ depends to some extent on what other spin configurations are in our set $\{|\alpha\rangle\}$ (our internal space). To illustrate this point, consider the following situation: suppose we have picked two configurations $|\alpha_1\rangle$ and $|\alpha_2\rangle$ from our configuration set $\{|\alpha\rangle\}$ and suppose we have to throw away one of them, so we must decide whether we want to keep $|\alpha_1\rangle$ or $|\alpha_2\rangle$. If the difference in energy of these two states is very large, for example take $|\alpha_1\rangle$ to be the Néel state and $|\alpha_2\rangle$ the state with $S_z^{\text{tot}}=0$ and with the largest number of ferromagnetic bonds, then one should clearly keep the lowest energy state, independently of what other states are present in the set $\{|\alpha\rangle\}$. But now suppose that $|\alpha_2\rangle$ has somewhat higher energy than $|\alpha_1\rangle$. The contribution of any given configuration from outside the set to a given

state which is a linear combination of the states in the set is not to be judged by simply looking at how far its energy lies from the energy of the state. As it will become clear in the following parts of the paper, what matters is the ratio of the Hamiltonian matrix element between the configuration and the state to their energy difference. That implies that if the coupling of $|\alpha_2\rangle$ to the whole set $\{|\alpha\rangle\}$ is larger to that of $|\alpha_1\rangle$ to the whole set, then it might be preferable to keep the configuration $|\alpha_2\rangle$, despite its higher energy.

Let $\{|\alpha\rangle\}$ denote the set of N_s configurations retained (internal space⁶), $|\psi^{(0)}\rangle$ the variational ground state in the $\{|\alpha\rangle\}$ subspace of energy $E^{(0)}$, and $\{|\beta\rangle\}$ the set of states not retained (external space⁶). We have implemented in this work the following adaptive state selection algorithm. We first estimate the correction $|\delta\psi\rangle$ from the external space to the approximate eigenstate $|\psi^{(0)}\rangle$ by first order perturbation theory, using as unperturbed Hamiltonian

$$\tilde{H}_0 = |\psi^{(0)}\rangle E^{(0)} \langle \psi^{(0)}| \quad (3a)$$

and

$$\tilde{H}_1 = H - \tilde{H}_0 \quad (3b)$$

as the perturbation. One thus has

$$|\psi^{(0)}\rangle \equiv \sum_{\alpha} c_{\alpha} |\alpha\rangle, \quad (4a)$$

$$|\delta\psi\rangle \equiv \sum_{\beta} c_{\beta} |\beta\rangle, \quad (4b)$$

where the coefficients $\{c_{\alpha}\}$ were obtained by diagonalizing the Hamiltonian in the internal space and we wish to estimate the coefficients $\{c_{\beta}\}$. To first order in \tilde{H}_1 , one has

$$c_{\beta} = \frac{1}{E^{(0)}} \sum_{\alpha} c_{\alpha} \langle \alpha | H | \beta \rangle. \quad (5)$$

Let M_s be the number of spin configurations in the external space which have nonzero matrix elements with any of the configurations $|\alpha\rangle$ in the internal space. The perturbative wave function $|\psi^{(1)}\rangle = |\psi^{(0)}\rangle + |\delta\psi\rangle$ is then a linear combination of $N_s + M_s$ states. We can now select a new internal space $\{|\alpha'\rangle\}$ by choosing the N_s configurations in $|\psi^{(1)}\rangle$ which have the largest (in magnitude) coefficients. To take full advantage of the variational freedom on the coefficients $\{c_{\alpha'}\}$, the wave function is relaxed, by diagonalizing the Hamiltonian in the new, improved internal space. The procedure can be repeated a number of times, until no further improvement in the ground state energy results. This algorithm does not always converge to a unique internal space $\{|\alpha\rangle\}$, since our state selection procedure is based on an approximate calculation of the effect of the external space. We have observed, in some cases, that the procedure oscillates between two sets of configurations. If one chooses one of the two sets, our state selection procedure picks as the new internal space the other set. After the wave function is relaxed, the state selection procedure gets us back to the original set. We have not found cases where the algorithm goes from set \mathcal{S}_1 to set \mathcal{S}_2 , to set \mathcal{S}_3 and then back to set \mathcal{S}_1 or more complicated limit cycles. This is not a serious practical problem, however, since in all the cases where these oscillations have occurred,

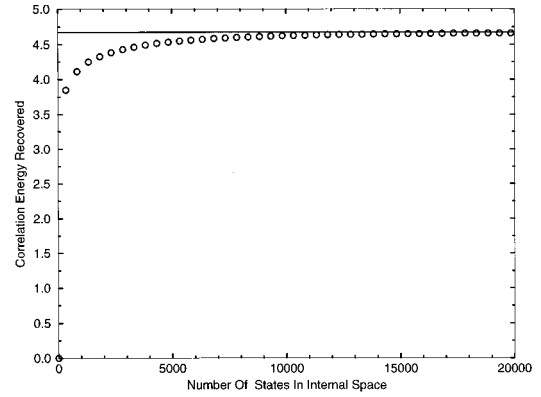


FIG. 1. The amount of correlation energy recovered as a function of the number of states kept in the internal space (circles) for the 24-site antiferromagnetic Heisenberg spin- $\frac{1}{2}$ chain in the $S_z^{\text{tot}} = 0$ and zero total momentum sector. The straight line is the exact result. The Hilbert space contains 112 720 states.

the difference in the variational ground state energy between the two possible internal spaces was in the fifth or sixth decimal place. One simply has to be careful to choose the appropriate termination criterion for the iterative procedure. We always save the previous internal space $\{|\alpha\rangle\}$ and the coefficients of the variational wave function $\{c_{\alpha}\}$ to disk. We stop iterating if the new internal subspace is identical to the old one or if the variational energy goes up from the previous iteration. In that case, we must discard the current wave function and retrieve the previous one from disk.

There is a vast number of variations of that simple algorithm that can be used. For instance, one need not truncate back to the same number N_s of states. One can use this procedure to increase the size of the internal space by n_s configurations, truncating to $N_s + n_s$ states in the state selection procedure. We have tried a few variants. Our experience is that internal spaces with lower variational energies are obtained if at every step of the adaptive state selection procedure the internal space changes little, i.e., if the search proceeds in small steps. Practically of course, some compromise must be made, since it obviously takes more computer time to find a near optimal solution if the search proceeds in very small steps.

Before we describe, and in order to motivate the second step of our method, it is interesting to calculate how much of the correlation energy, i.e., the difference between the exact ground state energy and the energy of the Néel state, one can recover as a function of the number of states kept with the adaptive procedure we have just described.

The results are shown in Fig. 1, and were obtained as follows. For a number of states kept larger than 3344, we first kept all the states up to an energy 3 above the Néel state and used the adaptive algorithm to find a better set of 3344 configurations. Then the number of configurations was increased by 500, and the set of configurations was optimized with the adaptive algorithm until the ground state energy could not be lowered anymore keeping the number of states fixed at 3844. The number of configurations was then increased by 500, and so on. For a number of states kept less than 3344, we started with our best internal space with 3344 configurations, discarded the 500 states with the smallest

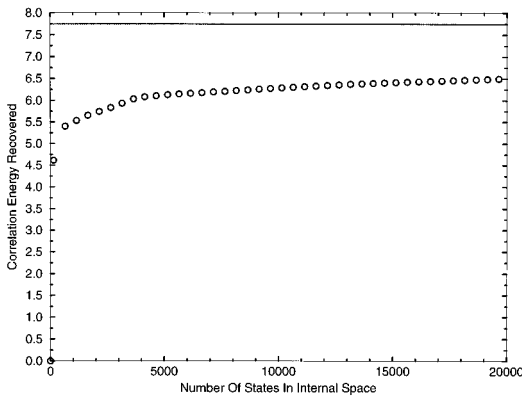


FIG. 2. The amount of correlation energy recovered as a function of the number of states kept in the internal space (circles) for the 40-site antiferromagnetic Heisenberg spin- $\frac{1}{2}$ chain in the $S_z^{\text{tot}} = 0$ and zero total momentum sector. The straight line is the exact result. The Hilbert space contains approximately 3.4×10^9 states.

weight in the wave function. We used the state selection method to improve on this initial internal space until the ground state energy could not be lowered anymore keeping the number of states fixed at 2844. The 500 configurations with the smallest weight in the wave function were discarded and so on until the number of configurations in the internal space was reduced to 344.

One can see from the figure that the initial rate of recovery of correlation energy as a function of the number of states kept is very fast. However, it is also clear from the figure that past 4000–5000 states kept, the recovery rate becomes exceedingly slow. One can see this even better for a larger spin chain. Figures 2 and 3 display our results for a 40-site and 60-site Heisenberg chain, which were obtained in a similar fashion as the results for the 24-site chain shown in Fig. 1, except that we initially started with all the states up to an energy 2 above the Néel state. It is striking that the amount of correlation energy missing at the point where the rate of recovery of correlation energy becomes exceedingly slow gets larger as the system size increases. Whereas one can easily recover about 95% of the correlation energy for

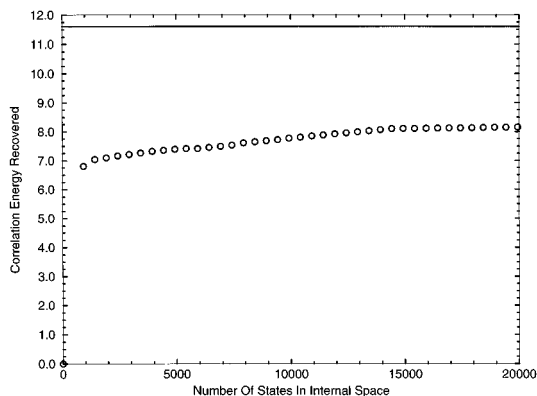


FIG. 3. The amount of correlation energy recovered as a function of the number of states kept in the internal space (circles) for the 60-site antiferromagnetic Heisenberg spin- $\frac{1}{2}$ chain in the $S_z^{\text{tot}} = 0$ and zero total momentum sector. The straight line is the exact result. The Hilbert space contains approximately 2×10^{15} states.

the 24-site chain with the adaptive state selection in real space we have described, that number is only about 80% for the 40-site chain and about 65% for the 60-site system. This underscores the incapacity of the real space procedure to yield all of the low-lying states of the system. This indicates that we must change the strategy of state selection to accelerate the convergence rate. This is going to be our next step which is explained in the next section.

Before we introduce the improvement on our method, let us discuss some of the reason for the shortcomings of the real space method. The number of spin configurations with a given excitation energy, say 3 above the Néel state, increases exponentially with the size of the system. For instance in Table I, we see that there are 3344 configurations with an energy 3 above the Néel state for a 24-site chain. That number is 55 233 for a 40-site chain. Since it is better to keep states at an energy, say 3 above the Néel state than to keep states at an energy, say 9 above the Néel state (it is only when the states are relatively close in the energy that the choice is not obvious), and because of the exponential increase in the number of states with energy and system size, the state selection procedure eventually gets stuck at some maximum excitation energy for these larger systems, which corresponds to some maximum number of nearest-neighbor spin flips. Thus only correlations up to some length scale, significantly smaller than the system size for these larger, 40-site and 60-site systems can be taken into account in the real space, adaptive state selection procedure, and the missing correlation energy comes from the spin correlations on larger length scales. We thus expect, as the results displayed in Figs. 1–3 demonstrate, that the number of missing low-lying states increases as the size of the system increases. One would also expect that the gap from the approximate ground state that results from the real space step of our method to these other low-lying states gets smaller as the system size increases.

The lowest energy states obtained by diagonalizing the Hamiltonian in the internal space generated by the adaptive state selection procedure are completely decoupled. Since it would require adding an exponentially larger number of higher energy spin configurations to significantly improve on this initial step, the best strategy given finite computational resources is to generate new low-energy states that couple to the correlated wave functions we have obtained and are linearly independent of them. If one has some knowledge about the collective modes, or long wavelength modes in the system, one can explicitly construct such low-lying states from the correlated states obtained by diagonalizing the Hamiltonian in the internal space.

One further comment about the excitation spectrum is in order. Whereas our results for the ground state energy E_0 are variational, those for the excitation spectrum, i.e., the differences $E_i - E_0$ for the excited states of energy E_i , $i = 1, 2, 3, \dots$, are not. We found that for a given computational effort (number of states retained), one gets better results for the correlation energy than for the first excited state, although not by a lot in this rather small size system. It is due to the fact that for the 24-site chain we do not have really long wavelength fluctuations. The energy difference of about 0.7 between the first excited state and the ground state, indi-

TABLE II. Comparison of configuration sets.

Energy	Number of states without state selection	Number of states with state selection
-6	1	1
-5	11	11
-4	305	275
-3	3027	1500
-2	0	1386
-1	0	171

states that the excitation is rather local. This is clearly seen in the expectation value of $N^{-1}\sum_i \mathbf{S}_i \cdot \mathbf{S}_{i+l}$, $l=1, \dots, N$ in the two states. In a larger system, the long wavelength part of the excitation spectrum obtained with this real space method alone would be even a poorer approximation to the correct low-lying spectrum.

Among the large number of variations in the adaptive state selection algorithm, the internal space for the 24-site chain used as a starting point for the momentum space step of our method was obtained as follows: we first kept all the states up to an energy 3 above the Néel state, a total of 3344 states, and used the adaptive procedure described above to select a better set of 3344 states. We have not tried, in this particular case, to start with a smaller set of configurations and increase the number of states kept progressively. In Table II, we compare the configuration sets obtained by keeping all states up to an energy 3 above the Néel state and the internal space that results when the state selection technique is applied. The difference is quite striking, about half of the states at an energy 3 above the Néel state are discarded in favor of higher excited states, and the percentage of the correlation energy recovered goes from 89.7% to 95.5%. Since we cannot find all the eigenvectors in the internal space, we only keep the n correlated states of lowest energy, with n much smaller than 3344, the dimension of the internal space. In this work, we have used $n=20$ correlated states.

DESCRIPTION OF LONG-RANGE CORRELATIONS

The next step in the method is designed to correct the long wavelength behavior of the wavefunction by carefully selecting the excited states that are retained in the calculation. The energy of a given state is simply the number of lattice sites N times the expectation values of $\mathbf{S}_i \cdot \mathbf{S}_{i+1}$, for any i . It only involves nearest neighbor spin correlations. Two eigenstates that differ very little in energy will exhibit very similar short-range spin correlations and thus will only be significantly different (they have to be orthogonal) for long range correlations. Since the Hamiltonian is local, namely only couples directly nearest-neighbor spins, the correlation (or equivalently, interaction) of spins that are far apart involves high orders of perturbation theory and thus the highly excited states contribute more significantly to the low-lying excitation spectrum than to the local properties. Let us denote $\{|\Phi_i\rangle\}_{i=0}^{n-1}$ the lowest n correlated states obtained by diagonalizing the Hamiltonian in the internal subspace using the adaptive state selection method detailed earlier. We generate new states by using the following two-magnon correlation operators:

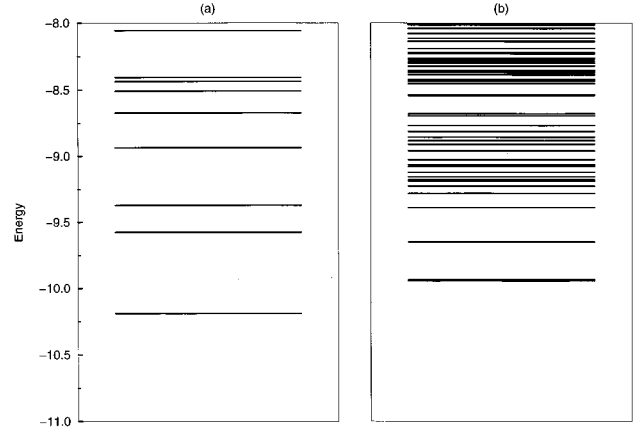


FIG. 4. (a) Energy of the states $\{|\Phi_i\rangle\}_{i=0}^{n-1}$ up to -8 . The internal space was generated without the adaptive state selection. All spin configurations below or at an energy 3 above the Néel state were kept. (b) Energy of the states $\{O_c(q)|\Phi_i\rangle\}_{i=0}^{n-1}$, $\{O_s(q)|\Phi_i\rangle\}_{i=0}^{n-1}$ for all wave vectors q up to an energy of -8 . The two lowest states are almost degenerate and are difficult to separate in the figure. They correspond to $O_c(q=\pi)|\Phi_0\rangle$ and $O_c(q=11\pi/12)|\Phi_0\rangle$ where $|\Phi_0\rangle$ is the lowest state in (a). The third lowest state is $O_c(q=5\pi/6)|\Phi_0\rangle$. The other states $O_c(q=\pi)|\Phi_i\rangle$, $i=2,3$, etc. are higher in energy as are the states $O_c(q)|\Phi_i\rangle$, $q=3\pi/4, 2\pi/6, \dots$

$$O_c(q) \equiv \sum_{l=0}^{N-1} \cos(ql) \sum_{m=1}^N S_{l+m}^+ S_m^-, \quad (6a)$$

$$O_s(q) \equiv \sum_{l=0}^{N-1} \sin(ql) \sum_{m=1}^N S_{l+m}^+ S_m^-, \quad (6b)$$

where $q=2\pi i/N$, $i=0, \dots, N/2$. Then, one carries out a variational calculation in the space spanned by

$$\{|\Phi_i\rangle\}_{i=0}^{n-1}, \quad \{O_c(q)|\Phi_i\rangle\}_{i=0}^{n-1}, \quad \{O_s(q)|\Phi_i\rangle\}_{i=0}^{n-1}$$

for all $0 \leq q \leq \pi$, and with, obviously, only $\{O_c(q)|\Phi_i\rangle\}_{i=0}^{n-1}$ when $q=0$ or π . Since one has $N/2+1=13$ wave vectors q , the size of the generalized eigenvalue problem that must be solved (the states are not orthogonal to one another) is $[2(N/2+1)-2+1]n=25n$.

The low-energy spectrum of the states $\{|\Phi_i\rangle\}_{i=0}^{n-1}$, $\{O_c(q)|\Phi_i\rangle\}_{i=0}^{n-1}$, $\{O_s(q)|\Phi_i\rangle\}_{i=0}^{n-1}$ is shown in Figs. 4 and 5. In Fig. 4, the results were obtained without the adaptive state selection procedure, namely the internal space was generated using an energy cutoff only. Figure 5 shows the corresponding results using the improved internal space, generated with the adaptive algorithm. Figures 4(a) and 5(a) show the low-lying spectrum of the states obtained with the real space method $\{|\Phi_i\rangle\}_{i=0}^{n-1}$ while Figs. 4(b) and 5(b) show the low-lying spectrum of the states $\{O_c(q)|\Phi_i\rangle\}_{i=0}^{n-1}$ and $\{O_s(q)|\Phi_i\rangle\}_{i=0}^{n-1}$. The two figures are remarkably similar [the lowest two states in Fig. 4(b) are almost degenerate whereas there is a larger gap in Fig. 5(b)], and show explicitly the failure of the real-space approach to generate all of the low-lying states in the system. In particular, the three states that have an energy between that of $|\Phi_0\rangle$ and $|\Phi_1\rangle$, the two lowest states produced by the real-space procedure, are in order of lowest energy, $O_c(q=\pi)|\Phi_0\rangle$,

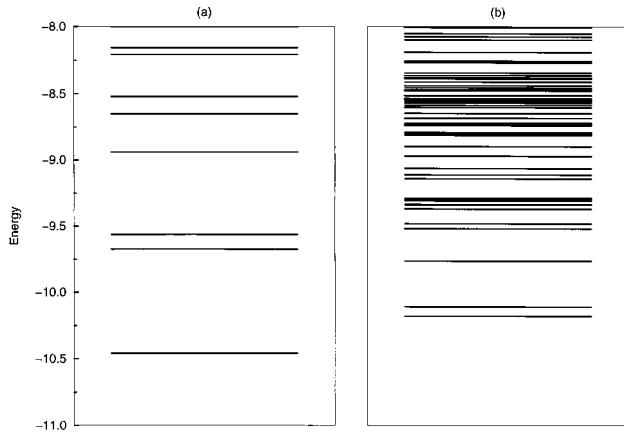


FIG. 5. (a) Energy of the states $\{|\Phi_i\rangle\}_{i=0}^{n-1}$ up to -8 . The internal space was generated with the adaptive state selection, as described in the text. (b) Energy of the states $\{O_c(q)|\Phi_i\rangle\}_{i=0}^{n-1}$, $\{O_s(q)|\Phi_i\rangle\}_{i=0}^{n-1}$ for all wave vectors q up to an energy of -8 . The two lowest states are better separated than in Fig. 4(b) and correspond to $O_c(q=\pi)|\Phi_0\rangle$ and $O_c(q=11\pi/12)|\Phi_0\rangle$, where $|\Phi_0\rangle$ is the lowest state in (a). The third lowest state is $O_c(q=5\pi/6)|\Phi_0\rangle$.

$O_c(q=11\pi/12)|\Phi_0\rangle$, and $O_c(q=5\pi/6)|\Phi_0\rangle$. These low-energy states couple to both $|\Phi_0\rangle$ and $|\Phi_1\rangle$ and thus do change the excitation spectrum significantly. Moreover, since they are at an energy below the first excited state produced by the real-space procedure, the excitation spectrum obtained in the first step of the method is thus totally unreliable. It is only when the states neglected in the calculation have an energy high relative to the low-lying states we are interested in that they do not alter qualitatively the low-lying spectrum, since their effect is to shift all the low-lying states by essentially the same amount. Because there are more wave vectors q in a larger system and they are more closely spaced, we would expect there would be even more states $\{O_c(q)|\Phi_i\rangle\}_{i=0}^{n-1}$ and $\{O_s(q)|\Phi_i\rangle\}_{i=0}^{n-1}$ very close to the lowest states $|\Phi_0\rangle$ and thus we would expect the correlation energy recovered in the second step of the method to increase as the size of the system gets larger. Note also that since there are more of these low-lying states in higher dimensions, and since the adaptive state selection procedure would produce a better starting point in two or three dimensions, we expect this method to be better suited to the study of correlated many-body systems in two or three dimensions.

Some comments are now in order. Whereas the states in adjacent entries in Table I can be obtained from each other by applying local operators, as was mentioned previously, the correlation operators in Eqs. (6a) and (6b) are nonlocal in space, in that they involve spins at any separation $l=0, \dots, N-1$. Suppose that the states $\{|\Phi_i\rangle\}_{i=0}^{n-1}$ obtained by the adaptive state selection procedure contain states with energies up to E_{\max} above the Néel state. By applying the correlation operators to the $|\Phi_i\rangle$ one generates states with energies up to $E_{\max}+2$ above the Néel state. To generate these types of configurations with the local, real space adaptive procedure would require much more computational resources.

The procedure of generating new states by applying operators to approximate eigenstates obtained in a previous step or iteration is similar to Wilson's renormalization group

approach to the Kondo problem.¹ The operators used by Wilson however have properties that do not generalize to the present situation. Their Hermitian conjugates annihilate the correlated states and their commutation relations were simple. This allowed Wilson to carry out an unlimited number of iterations while only keeping track of the matrix representations of relatively few operators.

We could imagine diagonalizing the Hamiltonian in the space spanned by $\{|\Phi_i\rangle\}_{i=0}^{n-1}$, $\{O_c(q)|\Phi_i\rangle\}_{i=0}^{n-1}$, $\{O_s(q)|\Phi_i\rangle\}_{i=0}^{n-1}$ and then truncating to the lowest n states, say $\{|\Phi'_i\rangle\}_{i=0}^{n-1}$ and generating new states by applying the correlations operators to the $|\Phi'_i\rangle$'s and so on, by analogy with Wilson's approach to the Kondo problem.¹ However, in order to carry out these renormalization steps, we need matrix elements of increasingly long strings of operators $O_c(q)$, $O_s(q)$ between our $|\Phi_i\rangle$'s. Since the computation of these matrix elements is the most time consuming step of the algorithm and the complexity of the computation increases rapidly with the length of the operator strings, there is a practical limit to the number of renormalization group iterations that can be carried out. However, this is not such a high price to pay, since we are starting from highly correlated states, and only a very few iterations are needed to obtain excellent results. We have only carried out one iteration, and this is already enough for the 24-site Heisenberg chain. It may be possible, using all symmetries and clever tricks, to carry out two such iterations for realistic problems, since the time consuming part of the method, generating the states $\sum_m S_{l+m}^+ S_m^- |\Phi_i\rangle$, $l=0, \dots, N-1$, $i=0, \dots, n-1$, can be done completely in parallel, and thus can be implemented very effectively on massively parallel supercomputers. This is another attractive feature of the method. Instead of the Wilson RG procedure described above, we could also generate a correlated basis

$$\begin{aligned} & \{|\Phi_i\rangle\}_{i=0}^{n-1}, \quad \{O_c(q)|\Phi_i\rangle\}_{i=0}^{n-1}, \\ & \{O_s(q)|\Phi_i\rangle\}_{i=0}^{n-1}, \quad \{O_c(q)O_c(q')|\Phi_i\rangle\}_{i=0}^{n-1}, \\ & \{O_s(q)O_c(q')|\Phi_i\rangle\}_{i=0}^{n-1}, \end{aligned}$$

etc. and use the adaptive state selection algorithm detailed earlier to retain a near optimal subset of such states. But once again, the computational complexity of calculating the states generated by applying long strings of correlation operators limits what can be done in practice.

The results of the variational calculation in the space spanned by the states $\{|\Phi_i\rangle\}_{i=0}^{n-1}$, $\{O_c(q)|\Phi_i\rangle\}_{i=0}^{n-1}$, $\{O_s(q)|\Phi_i\rangle\}_{i=0}^{n-1}$ are shown in Figs. 6 (no adaptive state selection) and 7 (with adaptive state selection), where they are compared to the exact results and to the results obtained with the real space step only. The two figures are again remarkably similar. The state selection procedure affords a better description of ground state correlations, and may undoubtedly yield larger benefits for a system whose Hilbert space is considerably larger than the one we have been studying. The excitation spectrum up to an energy 1 above the ground state is well described in both cases where the momentum space step is used, and not as well without it. As noted earlier, in a larger system with genuinely long wavelength excitations, the improvement brought about by the momentum space step should be much more significant. At higher energy, the situ-

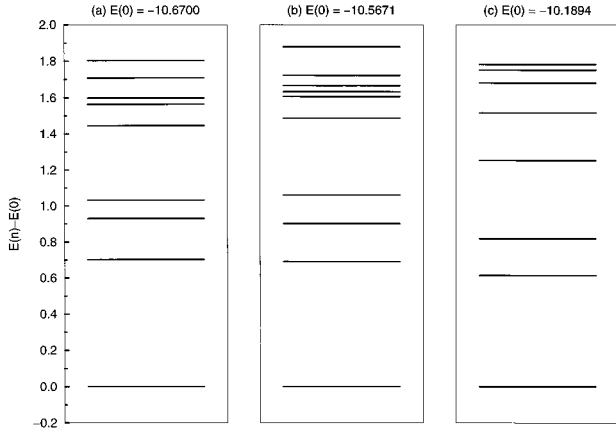


FIG. 6. (a) The exact result for the energy spectrum of the 24-site antiferromagnetic Heisenberg spin- $\frac{1}{2}$ chain in the $S^{\text{tot}}=0$ and zero total momentum sector. Also shown is the ground state energy $E(0)$. (b) The spectrum obtained with the present method, without using the adaptive state selection procedure. The internal space consists of the 3344 states with the lowest energy. $E(0)$ is the variational ground state energy. (c) The spectrum obtained without the momentum space step. $E(0)$ is the variational ground state energy obtained by diagonalizing the Hamiltonian in the space of the 3344 states of lowest energy.

ation degrades, but this is to be expected, since we have only carried out one RG iteration in momentum space. The states at energies above 1 would mix strongly with the states obtained by applying two correlation operators to the $\{|\Phi_i\rangle_{i=0}^{n-1}\}$ which would be in the same energy range. This brings us to a limitation of the method, namely the energy up to which the excitation spectrum is well described depends

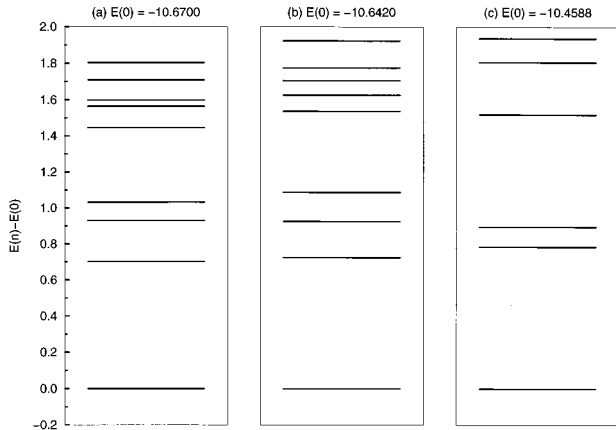


FIG. 7. (a) The exact result for the energy spectrum of the 24-site antiferromagnetic Heisenberg spin- $\frac{1}{2}$ chain in the $S^{\text{tot}}=0$ and zero total momentum sector. Also shown is the ground state energy $E(0)$. (b) The spectrum obtained with the present method using the adaptive state selection procedure. The internal space consists of the 3344 states with the largest coefficients in the trial ground state wave function chosen with the algorithm described in the text. $E(0)$ is the variational ground state energy. (c) The spectrum obtained without the momentum space step. $E(0)$ is the variational ground state energy obtained by diagonalizing the Hamiltonian in the optimized internal space of 3344 states selected by the adaptive algorithm.

on how high in energy the states obtained by applying two correlation operators lie. Only states below the energy of the lowest of these states can be correctly described. At higher energy, the results are unreliable.

We have been able to include all momenta q . This comes from the fact that the time consuming part of the calculation is the evaluation of the matrix elements such as $\sum_{m,m'} \langle \Phi_i | S_{l'+m}^- S_m^+ S_{l+m}^+ S_m^- | \Phi_j \rangle$ for all l and l' . Carrying out the Fourier transform for one q or all of them is an insignificant overhead. In this case we could have used instead the correlation operators

$$O(l) = \sum_{m=1}^N S_{l+m}^+ S_m^- \quad (7)$$

for $l=0, \dots, N-1$, namely the real space version of the operators $O_c(q)$ and $O_s(q)$ of Eqs. (6a) and (6b), and obtained the same answer. For larger systems, however, with many more wave vectors, it may not be possible to solve the generalized eigenvalue problem with dense overlap and Hamiltonian matrices that results when keeping all wave vectors. In that case it is better to do the calculation in momentum space with the operators $O_c(q)$ and $O_s(q)$ of Eqs. (6a) and (6b) and keep as many low-energy states as practical. Or better yet, one could select the appropriate states with an adaptive algorithm as we have use in the real space part of our method, but we have not implemented this idea in the present work.

It turns out that the states generated in the way described above are linearly dependent when keeping all wave vectors q . This is because the operator $O(l=0)$ of Eq. (7) acting on a state $|\Phi_i\rangle$ gives the number of up spins times the same state $|\Phi_i\rangle$ since all the configurations in the state $|\Phi_i\rangle$ have the same S_z^{tot} . This has the unfortunate effect of making the Cholesky decomposition of the overlap matrix in the solution of the generalized eigenvalue problem singular. This problem may also occur in larger systems, even when not all wave vectors are kept, but many correlated states are included. In this case some states may be nearly linearly dependent and the Cholesky decomposition may become unstable. In any event, when solving a generalized eigenvalue problem, it is a good idea to carry out a singular value decomposition of the overlap matrix to check for linear dependencies among the basis vectors. The overlap matrix S is decomposed as $S=UWV^T$, with U, V orthogonal matrices and W a diagonal matrix containing the singular values. We keep only as many singular values as is possible for a numerically stable solution to the eigenvalue problem, using the columns of the matrix U corresponding to the most important singular values as the new basis in which we carry out the diagonalization. If \mathbf{u}_i denotes the i th column of the matrix U , then the new overlap matrix \tilde{S} and Hamiltonian matrix \tilde{H} have matrix elements $\tilde{S}_{ij} = \mathbf{u}_i^T S \mathbf{u}_j$ and $\tilde{H}_{ij} = \mathbf{u}_i^T H \mathbf{u}_j$, respectively, where \mathbf{u}_i and \mathbf{u}_j are such that the singular values W_i and W_j are larger than some threshold ϵ . We have explicitly checked that the energy spectrum obtained by removing the small singular values when all wave vectors are kept agrees with the spectrum obtained with the same

method but discarding at the outset the states with $q=0$, which we know to be linearly dependent with the other states.

The accuracy of the results will of course depend on a judicious choice of the correlation operators. They must obviously not change the quantum numbers of the states $\{|\Phi_i\rangle\}_{i=0}^{n-1}$. They ought to be nonlocal in space to effectively correct the long-range behavior of the wave functions and must be chosen with some knowledge about the nature of the low-lying excitation spectrum. The long-range behavior of the ground state wave function determines the long wavelength dispersion relation of the collective modes in the system. Our choice of the correlation operators was motivated by the fact that the low-energy excitations are long wavelength magnons which can be obtained by applying a spin deviation operator in momentum space on the Néel state and that one needs two such magnons to preserve the magnetization and total momentum of the states. Including operators that create higher excitations, namely operators with more than one $S_i^+ S_j^-$ pair, would of course improve our results, especially the excitation spectrum at energies 1 above the ground state and higher as noted previously, but the complexity of the calculation of the matrix elements increases rapidly with the number of $S_i^+ S_j^-$ pairs, and this imposes practical limits on what can be done. This is not surprising, since including such operators is akin to carrying out more renormalization group iterations.

In ^4He , the linear in momentum part of the dispersion relation of the phonon spectrum is due to the long range behavior of the two-body correlation function, or equivalently the asymptotic behavior of the Jastrow correlation factor $f(r)$ as $r \rightarrow \infty$. However, the slope of the phonon spectrum, the sound velocity, does depend on the short-range correlations, and therefore a quantitative description of the excitation spectrum requires a good description of the short-range correlations as well as the proper asymptotic behavior of the wave functions.⁷

CONCLUSIONS

We have presented a technique to tackle the quantum many-body problem which combines the advantages of real

space RG ideas for the accurate description of the short-range correlations and of momentum space RG ideas to describe the long wavelength excitations. As a first step we have used a state selection method to find the best set of configurations holding their number N_s fixed. The correlation energy as a function of N_s can be separated in two regimes: The small N_s regime, where the energy changes rapidly toward the exact value with increasing N_s , and the large N_s regime where the energy changes very slowly with increasing N_s . Given finite computational resources, this requires a different approach if one wishes to obtain a yet better answer. To tackle this problem we have extended our state selection technique by using nonlocal operators to generate states in momentum space which accelerate the convergence and give us a much improved excitation spectrum. Therefore given any size system and any number of dimensions where one can apply the real space selection technique (of course restricting oneself to a finite number of states is a necessity), our technique can give a more accurate answer for the low-lying spectrum compared to a real space selection method alone. For example for the forty site problem we demonstrated in Fig. 2 that the state selection method becomes very slow for $N_s > 4000$. We found that for less computer time we can select much fewer states with the real space state selection method and then switch to momentum space step and find similar or better results for the energy of the low lying states.

We have made no special use of the one-dimensionality of the model problem we have studied. Therefore the prospects for applying the technique to higher dimensions are expected to be better than in one-dimensional lattice for the same dimensionality of the Hilbert space of the finite-size system studied. The reason being that quantum fluctuations are not as strong in higher dimensions.

ACKNOWLEDGMENTS

We should like to thank D. Pines, D. J. Scalapino, and J. R. Schrieffer for stimulating discussions on these and related topics. The research described in this paper has been supported in part by ONR (Grant No. N00014-93-1-0189) and by the National High Magnetic Field Laboratory.

¹K. G. Wilson, Rev. Mod. Phys. **47**, 773 (1975).

²S. Drell, M. Weinstein, and S. Yankielowicz, Phys. Rev. D **16**, 1769 (1977); J. Hirsch, Phys. Rev. B **22**, 5259 (1980); C. Dasgupta and P. Pfeuty, J. Phys. C **14**, 717 (1981); T. P. Zivkovic, B. L. Sandleback, T. G. Schmalz, and D. J. Klein, Phys. Rev. B **41**, 2249 (1990); M. B. Lepetit and E. Manousakis, *ibid.* **48**, 1028 (1993).

³S. R. White, Phys. Rev. B **48**, 10 345 (1993); Phys. Rev. Lett. **69**, 2863 (1992).

⁴S. R. White, Phys. Rev. B **45**, 5752 (1992).

⁵S. Liang, Phys. Rev. Lett. **75**, 3493 (1995).

⁶W. Wentzel and K. G. Wilson, Phys. Rev. Lett. **69**, 800 (1992); M. M. Steiner, W. Wentzel, K. G. Wilson, and J. W. Wilkins, Chem. Phys. Lett. **231**, 263 (1994).

⁷R. P. Feynman and M. Cohen, Phys. Rev. **102**, 1189 (1956); E. Feenberg, *Theory of Quantum Fluids* (Academic, New York, 1969); E. Manousakis and V. R. Pandharipande, Phys. Rev. B **30**, 5062 (1984).

⁸C. W. Murray, S. C. Racine, and E. R. Davidson, J. Comput. Phys. **103**, 382 (1992).